

Manifold-driven spirals in N-body barred galaxy simulations

E. Athanassoula

Aix Marseille Université, CNRS, LAM, UMR 7326, 13388 Marseille 13, France, e-mail: lia@oamp.fr

Accepted . Received -

ABSTRACT

We discuss the properties of spiral arms in a N-body simulation of a barred galaxy and present evidence that these are manifold-driven. The strongest evidence comes from following the trajectories of individual particles. Indeed, these move along the arms while spreading out a little. In the neighbourhood of the Lagrangian points they follow a variety of paths, as expected by manifold-driven trajectories. Further evidence comes from the properties of the arms themselves, such as their shape and growth pattern. The shape of the manifold arms changes considerably with time, as expected from the changes in the bar strength and pattern speed. In particular, the radial extent of the arms increases with time, thus bringing about a considerable increase of the disc size, by as much as 50% in about a Gyr.

Key words: galaxies: spiral – galaxies: structure – galaxies: kinematics and dynamics – galaxies: evolution.

1 INTRODUCTION

In a series of papers (Romero-Gómez et al. 2006, Paper I; Romero-Gómez et al. 2007, Paper II; Athanassoula, Romero-Gómez & Masdemont 2009a, Paper III; Athanassoula et al. 2009b, Paper IV; Athanassoula et al. 2010, Paper V), we proposed a theory to explain the formation and properties of spirals and inner and outer rings in barred galaxies. According to it, the backbone of these structures are a bunch of orbits guided and confined by the invariant manifolds associated with the periodic orbits around the saddle points of the potential in the frame of reference co-rotating with the bar. We call our theory manifold theory, or manifold flux-tube theory.

Some of the introductory dynamics necessary to follow our work is summarised in (Binney & Tremaine 2008, Sect. 3.3.2). Manifolds and the orbits they guide are described and explained in Paper I, while a relatively lengthy summary, avoiding equations, can be found in Sect. 2 of Paper III. Here we analyse a N-body simulation of an evolving barred galaxy and present evidence that its spiral arms are manifold-driven. In Sect. 2 we give a brief theoretical reminder and describe relevant manifold shapes in simple analytical potentials. In Sect. 3 and 4 we present the simulation and our results and make comparisons with our theoretical predictions. Further discussion and conclusions are given in Sect. 5.

2 THEORETICAL REMINDERS AND EXTENSIONS

Let us model a barred galaxy potential in the simplest possible way, namely by an axisymmetric part (including the disc and the halo) and a bar, which we assume rotates with a constant angular velocity. The dynamics of this system is best studied in a frame co-rotating with the bar, where there are five equilibrium points at

which the derivative of the potential in the rotating frame is zero. These are called Lagrangian points (L_i , $i = 1, 5$). Two of them (L_1 and L_2) are located on the direction of the bar major axis, outside the bar but near its ends. By convention, we place the bar along the x axis, measure the angles in a counterclockwise sense and call L_1 (L_2) the Lagrangian point on the right (left) of the centre. L_1 and L_2 are saddle-point unstable, so that the families of periodic orbits around each one of them (called Lyapunov orbits, Lyapunov 1949) are, at least in their neighbourhood, also unstable. They thus can not trap regular quasi-periodic orbits around them since any orbit with initial conditions in their immediate vicinity (in phase space) is chaotic and will have to escape their neighbourhood. Not all departure directions are, however, possible. The direction in which the orbit can escape is set by what are called the invariant manifolds.

Manifolds can be thought of as tubes that guide the motion of particles whose energy is equal to theirs. There are four manifold branches emanating from a given Lyapunov orbit (Fig. 2 of Paper III), two inside corotation (inner branches) and two outside (outer branches). Along two of these branches (one inner and one outer) the mean motion is towards the region of the Lagrangian point, while along the other two it is away from it. In Papers I – V we proposed that these manifolds and the orbits they guide are the building blocks of the spirals and rings in barred galaxies.

Fig. 1 illustrates a number of useful manifold shapes and properties. In the left panel, we use a potential including a spiral component. The latter exerts an additional gravitational forcing which is not symmetric with respect to the bar major axis, thus shifting the Lagrangian points away from that axis. The motion along the inner manifold branch (light green), is from the upper bar region to the left, i.e. towards the L_2 , as shown by the black arrow. These manifolds then circle for a few times around the L_2 and then follow the outer manifold branch (red), in the sense shown by the ar-

arXiv:1207.4590v1 [astro-ph.GA] 19 Jul 2012

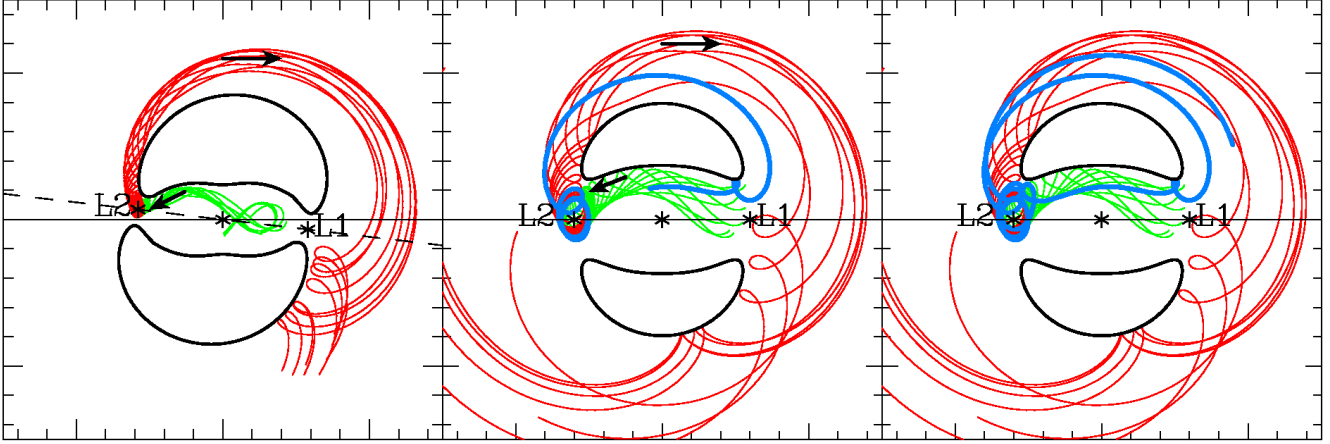


Figure 1. Manifolds related to the L_2 Lagrangian point in two simple analytical potentials. We plot in light green the inner manifold branch, in red the outer one and in blue a specific manifold (see text). In black we plot the zero velocity curve, and we mark by arrows the direction of the motion along the manifolds and with asterisks the positions of the L_1 , L_2 and the galactic centre. The thin black solid line indicates the direction of the bar major axis and the dashed one the direction joining the L_1 to the L_2 .

row, thereby outlining the spiral. After tracing somewhat more than 180° in azimuth, they form a loop each, as if they were bouncing off a circle with radius roughly equal to the outer distance of the zero velocity curve from the galactic centre. All displayed manifolds have the same Jacobi constant, near that of the L_1 and L_2 .

In the middle and right panels, we use a simple bar potential with no spiral component, so that the L_1 and L_2 are now on the direction of the bar major axis. The manifolds are very similar to those of the previous example, with one considerable difference, i.e. we chose now to display manifolds whose Jacobi constant is much larger than that of the L_1 and L_2 . Therefore, both the Lyapunov orbits and the outline of the corresponding manifolds are much larger than in the previous example (see also Paper I) and part of the outer (red) manifolds, when reaching the vicinity of L_1 will turn inwards, becoming inner manifolds and moving leftwards along the upper part of the bar towards the L_2 . We plot, in blue, one of these manifolds as an illustration. Note that amongst all the red manifolds, the one that turns inwards is the one which is leftmost in the last part before reaching L_1 . This motion is characteristic of manifolds with relatively large Jacobi constant and is explained in detail in Koon et al. (2000) and in Paper II (cf. also Paper V). The fraction of orbits that follows such trajectories depends on the potential and the distribution function of the orbits. In the right panel we follow the evolution of the blue manifold further to later times and show that it retraces the upper outer manifold branch. Another alternative (not shown here) is that, in the neighbourhood of the L_2 , instead of going upwards and following the arm, the trajectory goes downwards and follows an inner branch below the bar major axis (as e.g. in Fig. 1 of Paper 5, or the black path in the left panel of Fig. 3 in that paper, albeit for a different potential).

3 SIMULATION

The simulation we will discuss here has two live components, a halo and a disc, represented by a million and 200 000 particles, respectively. The former has a volume density

$$\rho_h(r) = \frac{M_h}{2\pi^{3/2}} \frac{\alpha}{r_c} \frac{\exp(-r^2/r_c^2)}{r^2 + \gamma^2},$$

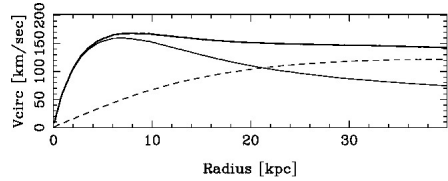


Figure 2. Model rotation curve (thick solid line). The halo and disc contributions are given by a dashed and a thin solid curve, respectively.

where r is the radius, M_h is the halo mass, γ and r_c are the halo core and cut-off radii, respectively, and the constant α is given by $\alpha = [1 - \sqrt{\pi} \exp(q^2) (1 - \text{erf}(q))]^{-1}$, where $q = \gamma/r_c$ (Hernquist 1993). We use here $\gamma = 15$ kpc, $r_c = 50$ kpc and $M_h = 25 \times 10^{10} M_\odot$. The initial density distribution of the disc is

$$\rho_d(R, z) = \frac{M_d}{4\pi h^2 z_0} \exp(-R/h) \text{sech}^2\left(\frac{z}{z_0}\right), \quad (1)$$

where R is the cylindrical radius, M_d is the disc mass, h is the disc radial scale length and z_0 is the disc vertical scale thickness. We use here $h = 3$ kpc, $z_0 = 0.6$ kpc and $M_d = 5 \times 10^{10} M_\odot$. The corresponding rotation curve is shown in Fig. 2. For the radial velocity dispersion of the disc particles, $\sigma_R(R)$, we take $\sigma_R(R) = 100 \cdot \exp(-R/3h)$ km s $^{-1}$.

The initial conditions were made using the iterative method (Rodionov, Athanassoula & Sotnikova 2009), and the simulation was run using the GADGET2 code (Springel, Yoshida, & White 2001; Springel 2005). We adopted softening lengths of 100 (200) pc for the disc (halo) and an opening angle of 0.5.

4 RESULTS

To follow the morphological evolution in this simulation, we saved the snapshots every 0.005 Gyrs. For each one of them, the position angle of the bar was calculated and the snapshot rotated so as to display the bar horizontally. In this manner, we visualise the evolution in a frame of reference co-rotating with the bar. An animation, using these frames and produced with the GLNEMO2 software, can be viewed in <http://195.221.212.246:4780/dynam/movie/MFolds>,

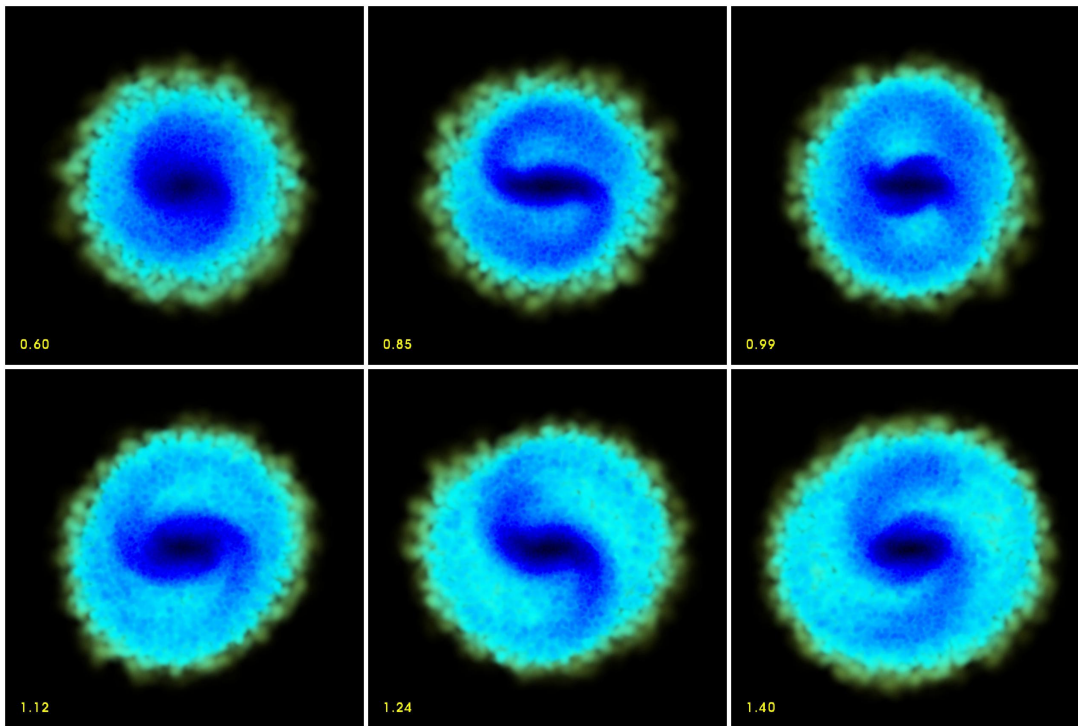


Figure 3. Evolution of the disc component. The time in Gyrs is given in the bottom left corner of each panel.

sgs058_noorbits.avi and sgs058_polar.avi for face-on Cartesian and polar views, respectively, while selected frames are shown in Fig. 3.

For our initial conditions, and within a distance of the order of 20 kpc from the centre, the dynamics are dominated by the disc rather than the halo mass distribution. Because of this, the bar grows early-on in the simulation and fast in time. It is initially very fat, but by $t = 0.5$, it starts becoming longer and narrower, while two spiral arms start forming, one from each end of the bar. These spirals are trailing and their angular extent increases with time as their tip approaches the opposite side of the bar. Until about 0.9 or 1.0 Gyrs they form a grand-design two armed structure, staying attached to the end of the bar and rotating with the same pattern speed as the bar.

Shortly after $t = 0.9$ Gyrs, the shape of the bar undergoes strong changes – as material initially in the arms is accreted to its outer parts – while the arm-interarm density contrast drops, so that the spiral is not as clearly discernible. This is followed by a second spiral episode, qualitatively very similar to the first one and starting between 1.0 and 1.1 Gyrs. I.e. a new two-armed grand-design spiral develops, again starting from the tip of the bar and extending towards the opposite side of the bar. This second spiral episode lasts till about $t = 1.5$ Gyrs and its shape and amplitude are quantitatively considerably different from those in the first episode.

The above description is in good agreement with our manifold theory results. Indeed, this theory leads naturally to two-armed trailing spiral arms (Paper IV), which start growing from the tip of the bar first outwards and then towards the opposite end of the bar (Fig. 6, Paper I). Material for these arms should come from the outer parts of the bar (Paper V). One of the extremities of each arm should be linked to L_2 or L_2 , and the arms should rotate with the same pattern speed as the bar. All these developments and morphological properties are indeed seen during the evolution in our simulation, arguing strongly for a manifold origin of the spiral arms.

The main argument, however, in favour of the manifold origin of the spirals comes from the orbits of the individual particles. In density wave theory, the arms are loci of density maxima. Particles should thus traverse the arms, but stay longer in the arm than in the interarm region (Lin & Shu 1964). This is totally different from our manifold theory, where spiral arms should be a bundle of orbits guided by the manifolds, so that particles should move along the arms rather than across them.

It should thus be possible to find out which of the two theories is the main driver of the spiral structure in the simulation simply by following a number of particles. For this we use our series of snapshots in which the bar orientation is kept horizontal. At $t = 0.8$ Gyrs, when the bar and spiral are well developed, we selected 60 particles located in the part of the spiral arm which is near the tip of the bar, roughly where we estimated by eye that the L_2 Lagrangian point would lie (cf. left panel of Fig. 1). Similar results can be found by selecting particles at other times or locations, provided they are clearly in an arm at selection time. We then followed the trajectories of these particles from $t = 0.5$ to 1.55 Gyrs and produced a sequence of 211 frames in each of which we superposed on the snapshot of all disc particles a filled white circle marking the current location of each chosen particle and a white line for its trajectory over the previous 0.175 Gyrs¹. We repeated this task for all snapshots and thus produced an animation (http://195.221.212.246:4780/dynam/movie/MFolds_sgs058_orbits.avi and [sgs058_polar_orbits.avi](http://195.221.212.246:4780/dynam/movie/MFolds_sgs058_polar_orbits.avi) for Cartesian and polar views, respectively). In Fig. 4 we show nine such frames which display the salient features of the particle trajectories.

Roughly from $t = 0.5$ to 0.65 Gyrs the chosen particles travel

¹ This time range should be kept in mind when comparing the spiral shape and the early parts of orbit, because the spiral could have evolved during these 0.175 Gyrs.

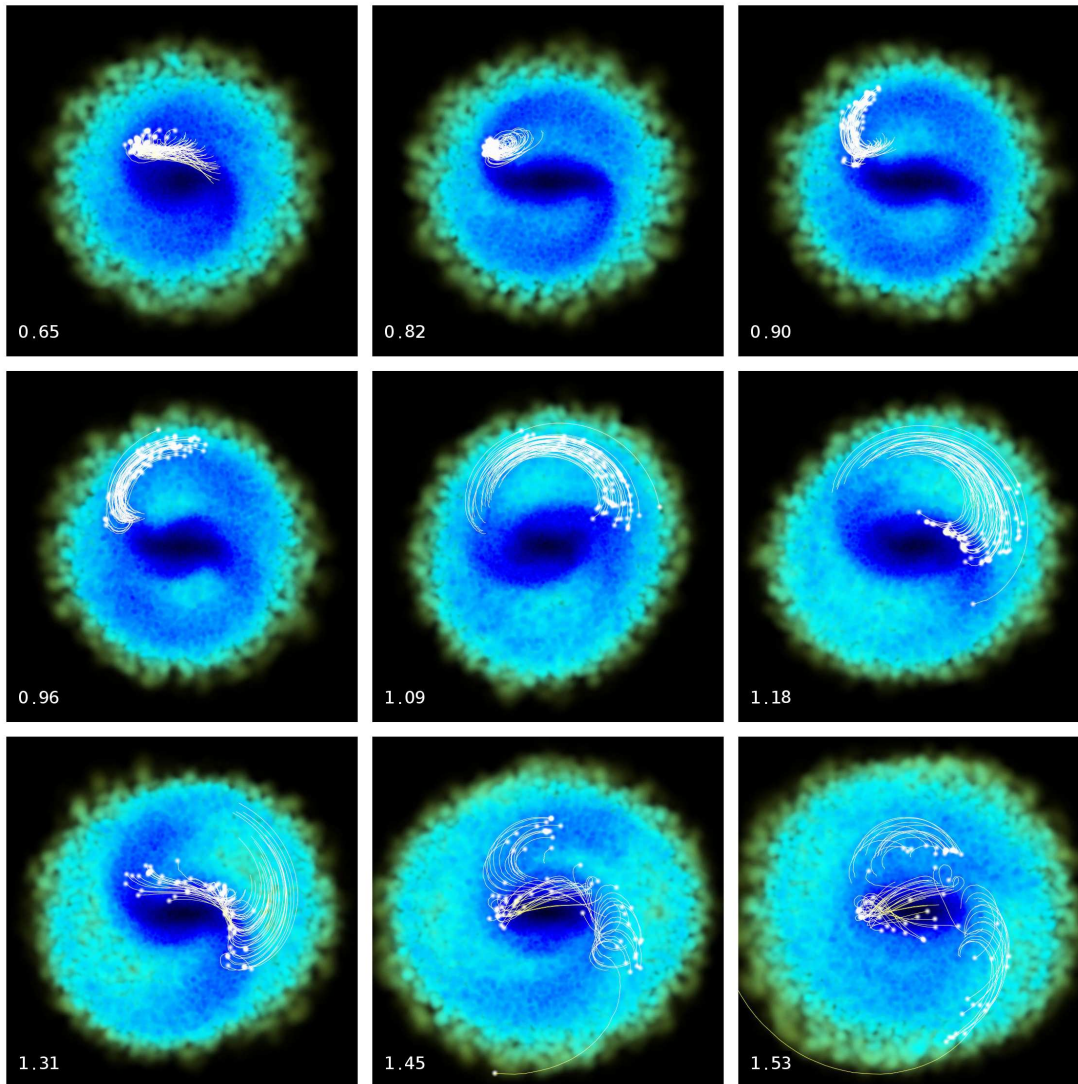


Figure 4. Nine snapshots of the disc component, on which we overlay the locations (white filled circles) and trajectories (white solid lines) of the 60 particles that we follow (see text). The time in Gyrs is given in the bottom left corner of each panel.

along the outer part of the bar, in the direction from the L_1 to the L_2 , then they circle a couple of times around what should be the L_2 (frame at $t = 0.82$) and escape its vicinity following the arm (times 0.90 to 1.18). Thus the particle orbits stay within the arms, as expected for the manifold theory, and do not cross them as would have been expected by the density wave theory. After roughly $t = 1.1$ Gyrs, the forerunners of the group of particles we follow reach the vicinity of the opposite side of the bar from which they emanated (i.e. the right side, near L_1). From that point onward the particles divide themselves into two groups. Some continue downwards, make a loop, as if they were bouncing off an invisible barrier, and then trace the *lower* spiral arm from the L_1 to the L_2 . Others retrace the upper outline of the bar leftwards in the direction from L_1 to L_2 . Once they have reached the vicinity of L_2 another branching occurs. Some particles go to the upper spiral arm which they follow from the L_2 to the L_1 , while others stay in the bar (frames at $t = 1.45$ and 1.53). All the trajectories and branch-

ings described above are very similar to those seen in Fig. 1 and in Papers I - V.

Furthermore, note that the orbits spread out as they trace the arm moving from the L_2 to the L_1 between $t = 0.65$ and 1.1 Gyrs, leading to a gradual widening of the spiral arm. This can be already seen in Fig. 3. This widening also is expected from the manifold origin of these arms (Fig. 1 here and Papers I and V). How much this widening depends on the potential, so that we can not compare Figs. 1 and 4 quantitatively.

5 DISCUSSION AND CONCLUSIONS

In this letter we followed the formation of spiral structure in a N-body simulation of a barred disc galaxy. We witness the formation of a short-lived and recurrent spiral structure, two episodes of which last over roughly 1 Gyr. In between these two episodes the spiral never quite vanishes, but its amplitude decreases consider-

ably. These spirals have the same properties as the manifold-spirals discussed in Papers I to V. We also followed the trajectories of particles in the arms and found that, contrary to what would have been expected for density wave spirals, they do not cross the arms but they move along them, starting off from the vicinity of one of the Lagrangian saddle points (L_1 or L_2) in the direction of the other one. Thus their trajectories outline the arms. In fact the whole of the trajectory contributes to the spiral structure and these spirals can be called flux-tube manifold spirals.

There are several more signs, tell-tale of a manifold origin. For example, particles which outline the spiral have their origin in the outer part of the bar and join the spiral via the vicinity of a point whose location is compatible with that of the saddle Lagrangian points (L_1 or L_2). Furthermore, they loop in the vicinity of that point before they follow the arm. Another tell-tale sign of the manifold origin of the arm is that in the vicinity of each Lagrangian point the particles split into two groups, the same in simulations and in simple orbital calculations.

From all the above it becomes clear that we are witnessing manifold-driven spirals in our simulation. This – together with the good agreement between manifold-driven and observed rings and spirals found in Papers IV and V and by Martínez-García (2012) – argues strongly that manifolds do play a role in spiral and ring formation. Manifolds, however, are not the only possible origin of such structures. Indeed, spirals have been witnessed also in other N -body simulations and interpreted in terms of other theories (Sellwood & Carlberg 1984; D’Onghia, Vogelsberger & Hernquist 2012; Grand, Kawata & Cropper 2012; Sellwood 2012). We already included a note of caution to this avail in Paper V.

Our comparison between N -body and theoretical manifolds must necessarily stay qualitative. As any orbital structure work, the manifold theory relies on a few simplifications, the most important of which is that the potential is time-independent in the frame of reference co-rotating with the bar. On the other hand, in simulations and in real galaxies the potential evolves with time, due to redistribution of angular momentum via the resonances (e.g. Lynden-Bell & Kalnajs 1972; Weinberg 1985; Athanassoula 2002, 2003). However, if this evolution is not too fast, it should not present a problem for our flux-tube manifold theory where the arm is constituted by the whole flow of material guided by the manifolds² and will only lead to a change of the manifold properties with time. Any secular change in the potential is expected to lead to a secular evolution of the manifold properties. Furthermore, our simulations show that, even when the rate of change is considerable, particle trajectories are still guided by manifolds, keep their characteristic signatures and obey the selection rules of permissible paths defined by them. Nevertheless, their shape and extent change as expected, while particles can get trapped or untrapped by these manifolds.

Such orbits as described here have also been witnessed as responses to applied analytical potentials (e.g. Danby 1965; Patsis 2006, Papers III & V), although links to manifolds were not necessarily made. To our knowledge, however, this is the first time that the manifold theory is tested in a realistic self-consistent N -body simulation by following the motion of individual particles³.

² This is not the case for the theory presented in e.g. Voglis, Tsoutsis & Efthymiopoulos (2008), or Harsoula, Kalapotharakos & Contopoulos (2011) which considers the loci of the apsidal manifold sections. It thus requires a quasi-stationary, non-evolving potential.

³ A previous attempt (Tsoutsis, Efthymiopoulos & Voglis 2008) used an unrealistic simulation, with no separate disc and halo components, just a single cylindrical-shaped component, with a vertical to horizontal size ratio

Nevertheless, the simulation discussed here is in no way unique; manifold-driven spirals can be seen in a large number of our simulations, some of which include gas, and will be discussed elsewhere.

Comparing the disc extent between times 0.5 and 1.5 Gyrs we see a considerable change, of the order of 50%, due to the spirals. This shows that the bar and the associated manifolds can drive the overall evolution of the disc significantly. We will explore this process further in future work.

ACKNOWLEDGEMENTS

We thank M. Romero-Gomez and A. Bosma for help and discussions, and J.C. Lambert for his splendid work with GLNEMO (<http://projets.oamp.fr/projects/glnemo2>).

REFERENCES

- Athanassoula E., 2002, *ApJL*, 569, L83
 Athanassoula E., 2003, *MNRAS*, 341, 1179
 Athanassoula E., Romero-Gómez M., Bosma A., Masdemont J.J. 2009b, *MNRAS*, 400, 1706 (Paper IV)
 Athanassoula E., Romero-Gómez M., Bosma A., Masdemont J.J. 2010, *MNRAS*, 407, 1433 (Paper V)
 Athanassoula E., Romero-Gómez M., Masdemont J.J. 2009a, *MNRAS*, 394, 67 (Paper III)
 Binney J., Tremaine S., 2008, *Galactic Dynamics*, 2nd edition, Princeton University Press, NJ
 D’Onghia E., Vogelsberger M., Hernquist L. 2012, arXiv:1203.5208
 Danby J.M.A. 1965, *AJ*, 70, 501
 Grand R.J.J., Kawata D., Cropper M. 2012, *MNRAS*, 421, 1529
 Harsoula M., Kalapotharako, C., Contopoulos G., 2011, *MNRAS*, 411, 1111
 Hernquist L., 1993, *ApJS*, 86, 389
 Koon W., Lo M., Marsden J., Ross, S. 2000, *Chaos*, 10, 427
 Li, C. C., Shu F. H.-S. 1964, *ApJ*, 140, 646
 Lyapunov A. 1949, *Ann. Math. Studies*, 17
 Lynden-Bell, D., Kalnajs A. J. *MNRAS*, 157, 1
 Martínez-García E. 2012, *ApJ*, 744, 92
 Patsis P., *MNRAS*, 369, L56
 Rodionov S. A., Athanassoula E., Sotnikova N. Y., 2009, *MNRAS*, 392, 904
 Romero-Gómez M., Masdemont J.J., Athanassoula E., García-Gómez C. 2006, *A&A*, 453, 39 (Paper I)
 Romero-Gómez M., Athanassoula, E., Masdemont J.J., García-Gómez C. 2007, *A&A*, 472, 63 (Paper II)
 Sellwood J.A., 2012, *ApJ*, 751, 44
 Sellwood J.A., Carlberg R. 1984, *ApJ*, 282, 61
 Springel V., 2005, *MNRAS*, 364, 1105
 Springel V., Yoshida N., White S. D. M., 2001, *NewA*, 6, 79
 Tsoutsis P., Efthymiopoulos C., Voglis N. 2008, *MNRAS*, 387, 1264
 Voglis N., Tsoutsis P., Efthymiopoulos C. 2008, *MNRAS*, 373, 280
 Weinberg M. D. 1985, *MNRAS*, 213, 451

of ~ 0.3 and a velocity dispersion larger than 100 km/sec, i.e. properties very different from those of a spiral galaxy.